Polymer 135 (2018) 142–153

Contents lists available at ScienceDirect

Polymer

journal homepage: www.elsevier.com/locate/polymer

Syntheses of aromatic polymers containing imidazolium moiety and the surface modification of a highly gas permeable membrane using the nanosheets

Yu Nagase [a, b, *], Botakoz Suleimenova [a], Chihiro Umeda [b], Kosuke Taira [a], Tatsuma Oda [a], Sayaka Suzuki [a], Yosuke Okamura [a, b, c], Shinichi Koguchi [d]

[a] Course of Industrial Chemistry, Graduate School of Engineering, Tokai University, 4-1-1 Kitakaname, Hiratsuka, Kanagawa 259-1292, Japan
[b] Course of Applied Science, Graduate School of Engineering, Tokai University, 4-1-1 Kitakaname, Hiratsuka, Kanagawa 259-1292, Japan
[c] Micro/nano Technology Center, Tokai University, 4-1-1 Kitakaname, Hiratsuka, Kanagawa 259-1292, Japan
[d] Department of Chemistry, School of Science, Tokai University, 4-1-1 Kitakaname, Hiratsuka, Kanagawa 259-1292, Japan

ARTICLE INFO

Article history:
Received 16 October 2017
Received in revised form
30 November 2017
Accepted 4 December 2017
Available online 5 December 2017

Keywords:
Imidazolium-containing polyimide
Surface coating
Gas separation

ABSTRACT

Novel aromatic diamine monomer containing imidazolium group were synthesized to prepare polyimides and polyamide containing ionic liquid structure in the side chain by the polycondensation of the monomer with acid dianhydride or acid chloride. The glass transition temperatures, *Tg*, of the obtained polymers were in the range of 60–150 °C, and they exhibited the thermal stability up to 300 °C. The self-standing ultrathin films, so called nanosheets, of these aromatic polymers could be successfully prepared by spin-coating method. Then, the surface coating on the highly gas permeable membrane composed of polydimethylsiloxane graft copolyimide was carried out using the obtained nanosheets, and the effect of surface structure on the gas permeability and selectivity was investigated. As a result, the nanosheet coating on the highly gas permeable membrane with these polyimides containing imidazolium group was effective to improve the selectivity of CO_2/N_2 and O_2/N_2.

1. Introduction

The gas separation technology using polymer membranes has gathered much attention since they have a possibility to solve the energy and environmental problems [1–8]. Especially, the technology of CO_2 capture and storage (CCS) has been paid considerable attention for the reduction of CO_2 from the industrial waste gases to avoid the global warming. Therefore, several polymers have been developed as materials for CO_2 separation membranes. Lin and Freeman have reported that ethylene oxide units in the polymer appeared to be one of the useful groups to achieve the high CO_2 permeability and the high CO_2/light gas selectivity [9]. In addition, Okamoto et al. have studied PEO-segmented polyamides, and observed the CO_2 permeability coefficient at 58 Barrer and the separation factor of CO_2/N_2 at 53 [10]. Xiao et al. have developed a new type of polymers with intrinsic microporosity, which showed a high gas permselectivity [11]. Jiang et al. have also reported a CO_2-philic membrane consisting of semi-interpenetrating networks with oligo(ethylene oxide), which exhibited a high CO_2 permselectivity [12].

On the other hand, room-temperature ionic liquids such as imidazolium salts have attracted great interest because of their unique properties such as nonvolatile property, high thermal stability, high ionic conductivity and tunable solvation properties [13]. Recently, it is also worth noting that the ionic liquids are promising as new CO_2 separation media because ionic liquids exhibits preferential solubility for CO_2 over other light gases [14–19]. Moreover, the nonvolatile nature of ionic liquids prevents the loss of liquid during the separation process as compared with conventional liquid membranes. In order to introduce the affinity to CO_2 of ionic liquids into polymer membranes, several polymers containing imidazolium moiety have been synthesized to investigate the permselectivity of CO_2 against light gases [20–30]. Noble and his coworkers reported a lot of papers which described the syntheses

* Corresponding author. Course of Industrial Chemistry, Graduate School of Engineering, Tokai University, 4-1-1 Kitakaname, Hiratsuka, Kanagawa 259-1292, Japan.
E-mail address: yunagase@tokai-u.jp (Y. Nagase).

https://doi.org/10.1016/j.polymer.2017.12.016
0032-3861/

of polystyrenes and polymethacrylates having imidazolium salts and the preparations of crosslinked or photo-polymerized membranes for CO_2 separation [20–25]. Kammakakam et al. have reported the synthesis of alkyl imidazolium-functionalized cardo-based poly(ether ketone)s [26] or aromatic polyimides [27,28], which consisted of a rigid main chain, as membrane materials for CO_2 separation. It was also reported that the CO_2 permeability coefficient and the separation factor of CO_2/N_2 (PCO_2 and α) of the obtained poly(ether ketone) membrane were 1.19 Barrer and 66.1, respectively. Therefore, these imidazolium salt-containing polymer membranes exhibit good CO_2 separation performance owing to the good solubility of CO_2 on the imidazolium-rich surfaces, but PCO_2 is relatively low. On the contrary, Sakaguchi et al. have reported that polydiphenylacetylene containing imidazolium group exhibited the high CO_2 permselectivity [29,30], where PCO_2 and α reached at 11–53 Barrer and 44–31, respectively. Kharul et al. have also investigated main-chain type polybenzimidazole polymers *N*-quaternized by bulky substituents [31,32], which showed the similar CO_2 permselectivity.

In these years, we have investigated the highly gas permeable membranes based on polydimethylsiloxane (PDMS)-graft copolyamides and copolyimides [33–38]. Although the obtained polymers possessed a long PDMS segment in every repeating unit, the tough self-standing membranes could be prepared by a solvent casting method. Furthermore, the PDMS contents of PDMS-graft copolymers could be easily controlled by changing the PDMS segment length of the macromonomer. Then, the gas permeability coefficients of these graft copolymers were changed by PDMS segment length, but the separation factors of CO_2/N_2 was almost constant at 11–13. On the other hand, we focused on the processing for free-standing ultrathin films with a thickness less than 100 nm (so-called nanosheets), which exhibited the unique properties such as high adhesive strength, flexibility and smoothness [39]. If the nanosheets could be fabricated from the imidazolium-containing polymers and coated on the highly gas permeable membrane, the obtained composite membrane would exhibit the higher separation factor with maintaining a high permeability of CO_2.

In this study, we have attempted to synthesize novel aromatic polymers containing imidazolium groups in the side chain, and to fabricate the nanosheets composed of the obtained polymers. Then, the nanosheet-coating on the highly gas permeable PDMS-graft copolyimide membrane was carried out, and the effect of surface structure on the gas permeability and selectivity was investigated by the measurements of permeability coefficients of several gases through the nanosheet-coated composite membranes. If the separation factor of the specific gas could be improved by the surface modification using nanosheet-coating, a new type of highly permselective gas separation membrane would be developed.

2. Experimental

2.1. Materials

The synthetic procedures of hydrosilyl-terminated polydimethylsiloxane (PDMS-H) and 3,5-bis(4-nitro-3-methylphenoxy) benzoic acid (BNMPB) were described in our previous papers [33,40]. Tetrahydrofuran (THF) and toluene were distilled over sodium to remove a small amount of water. 4,4′-Oxydiphthalic anhydride (ODPA) and 4,4′-hexafluoropropylidene diphthalic anhydride (6FDA) were purchased from Tokyo Chemical Industry Co., Ltd. (Tokyo, Japan) and used as received. Other chemical reagents were used without further purification.

2.2. Syntheses of diamino-terminated PDMS macromonomer and PDMS graft copolyimide

2.2.1. Synthesis of 3-butenyl 3,5-bis(4-nitro-3-methylphenoxy) benzoate (**1**)

To a solution of BNMPB (10.0 g, 23.6 mmol) dissolved in 71 ml of 2-butanone, 4-bromo-1-butene (4.60 g, 34.1 mmol) and K_2CO_3 (4.70 g, 34.1 mmol) were added, and the mixture was refluxed for 22 h. Then, the organic products were extracted with chloroform, and purified by column chromatography on silica gel with ethyl acetate/hexane (1/2 v/v) to obtain 11.2 g of **1** as a white solid (Yield: 98.8%).

^{1}H NMR: δ (500 MHz, $CDCl_3$, ppm): 2.50 (2H, m), 2.62 (6H, s), 4.37 (2H, t, $J = 6.8$ Hz), 5.10 (2H, m), 5.81 (1H, m), 6.92 (4H, m), 6.98 (1H, t, $J = 2.5$ Hz), 7.55 (2H, d, $J = 2.5$ Hz), 8.08 (2H, d, $J = 8.5$ Hz).

2.2.2. Synthesis of 3,5-bis(4-nitro-3-methylphenoxy) benzoyloxybutyl-terminated PDMS (**2**)

PDMS-H (y = 12.1, 10.3 g, 10.2 mmol), **1** (4.08 g, 8.53 mmol) and Pt/C powder (5%, 0.333 g) were mixed in 11 ml of dry toluene under an argon atmosphere. Then, the mixture was stirred at 80 °C for 22 h. After the solvent was evaporated, the product was purified by column chromatography on silica gel with hexane/ethyl acetate (20/1 v/v) to obtain 9.32 g of **2** as a pale yellow liquid. (Yield: 73.8%, $m = 11.7$).

^{1}H NMR: δ (500 MHz, $CDCl_3$, ppm): 0.05 (6 *m*H, m), 0.45 (3H, t, $J = 3.5$ Hz), 0.49 (2H, t, $J = 12.3$ Hz), 0.81 (4H, t, $J = 6.5$ Hz), 1.37 (2H, m), 1.69 (2H, m), 2.54 (6H, s), 4.24 (2H, t, $J = 6.8$ Hz), 6.82 (1H, m), 6.84 (3H, s), 6.90 (1H, t, $J = 2.3$ Hz), 7.48 (2H, d, $J = 2.5$ Hz), 8.00 (2H, d, $J = 8.5$ Hz).

2.2.3. Synthesis of 3,5-bis(4-amino-3-methylphenoxy) benzoyloxybutyl-terminated PDMS (**3**)

The compound **2** (9.32 g, 6.38 mmol) was dissolved in 64 ml of ethanol, and Pd/C powder (5%, 0.271 g) was suspended in the solution. The mixture was degassed under reduced pressure at −78 °C, and the reaction vessel was purged with hydrogen over 101 kPa. Then, the mixture was stirred at room temperature for 42 h. After Pd/C powder was filtered off washing with ethanol, the solvent was evaporated under reduced pressure to obtain 8.75 g of **3** as a purple viscous liquid. (Yield: 97.9%, $m = 11.3$).

^{1}H NMR: δ (500 MHz, $CDCl_3$, ppm): 0.002 (6 *m*H, m), 0.48 (4H, m), 0.81 (3H, t, $J = 6.8$ Hz), 1.24 (4H, m), 1.35 (2H, m), 1.65 (2H, t, $J = 7.5$ Hz), 2.09 (6H, s), 4.18 (2H, t, $J = 9.5$ Hz), 6.65 (7H, m), 7.15 (2H, d, $J = 2.5$ Hz).

IR, ν (KBr, cm^{-1}): 3568 (-NH_2), 2963, 1717 (C=O), 1624, 1597, 1504, 1439, 1419, 1261 (Si-C), 1161, 1022 (Si-O-Si), 798.

2.2.4. Synthesis of PDMS graft copolyimide (***PIS12***)

The obtained PDMS macromonomer **3** ($m = 11.3$, 4.32 g, 3.19 mmol) was dissolved in 22 ml of anhydrous dimethylacetamide (DMAc) under an argon atmosphere. To this solution, the solution of ODPA (0.990 g, 3.19 mmol) dissolved in 22 ml of anhydrous DMAc was added dropwise. After the solution was stirred for 18 h at room temperature, 2.4 ml of acetic anhydride and 3.6 ml of triethylamine were added, and the mixture was stirred at 80 °C for 10 h. Then, the mixture was poured into excess methanol to precipitate the polymer. The obtained polymer powder was filtered and dried. The reprecipitation of the chloroform solution into methanol gave 4.17 g of **PIS12** ($m = 12.8$) as a pale brown powder. (Yield: 80.3%, $m = 12.4$).

^{1}H NMR: δ (500 MHz, $CDCl_3$, ppm): 0.002 (6 *m*H, s), 0.45 (2H, t, $J = 7.5$ Hz), 0.53 (2H, t, $J = 8.3$ Hz), 0.80 (3H, t, $J = 4.0$ Hz), 1.23 (6H, m), 1.72 (2H, t, $J = 7.3$ Hz), 2.14 (6H, s), 4.25 (2H, t, $J = 7.0$ Hz), 6.90 (2H, m), 6.95 (2H, s), 6.98 (1H, s), 7.12 (2H, d, $J = 8.5$ Hz), 7.43 (2H, d,

J = 7.5 Hz), 7.51 (4H, d, J = 14.0 Hz), 7.95 (2H, d, J = 8.0 Hz).

IR, ν (KBr, cm^{-1}): 2962, 2920 (C-H), 1730 (C=O), 1608, 1506, 1261 (Si-C), 1097 (Si-O-Si).

2.3. Syntheses of monomer compounds containing imidazolium group

2.3.1. Synthesis of 6-tosylhexanol

Under an argon atmosphere, 1,6-hexandiol (37.2 g, 315 mmol) and triethylamine (29.3 ml, 210 mmol) were dissolved in 44 ml of dry THF. Then, the solution of tosyl chloride (20.1 g, 105 mmol) dissolved in 30 ml of dry THF was added dropwise at 0 °C, and the mixture was stirred at room temperature for 17 h. After the mixture was poured into excess water, the organic product was extracted with chloroform, and purified by column chromatography on silica gel with ethyl acetate/hexane (1/1 v/v) to obtain 19.2 g of 6-tosylhexanol as a transparent colorless liquid (Yield: 67.0%).

^{1}H NMR: δ (500 MHz, DMSO, ppm): 1.19 (4H, m), 1.33 (2H, m), 1.54 (2H, m), 2.42 (3H, s), 2.50 (2H, m), 3.25 (2H, t, J = 6.5 Hz), 4.00 (2H, t, J = 6.3 Hz), 7.48 (2H, d, J = 8.0 Hz), 7.78 (2H, d, J = 8.0 Hz).

2.3.2. Synthesis of 6-tosylhexyl 3,5-bis(4-nitro-3-methylphenoxy) benzoate (**4**)

To the solution of BNMPB (12.6 g, 29.6 mmol) dissolved in 30 ml of chloroform, thionyl chloride (22.0 ml, 296 mmol) and 3 drops of dimethylsulfoxide (DMF) was added, and the mixture was refluxed for 2 h. Then, the organic solvents and the excess $SOCl_2$ were distilled off under reduced pressure to obtain 3,5-bis(4-nitro-3-methylphenoxy)benzoyl chloride as a yellow solid. Under an argon atmosphere, 6-tosylhexanol (9.17 g, 32.6 mmol) and triethylamine (8.25 ml, 59.2 mmol) were dissolved in 44 ml of dry THF. The obtained 3,5-bis(4-nitro-3-methylphenoxy)benzoyl chloride was dissolved in 30 ml of dry THF, and the solution was added dropwise. The mixture was stirred at room temperature for overnight. After the mixture was poured into excess water, the organic products were extracted with chloroform, and purified by column chromatography on silica gel with ethyl acetate/hexane (1/1 v/v) to obtain 15.2 g of **4** as a yellow viscous liquid (Yield: 75.6%).

^{1}H NMR: δ (500 MHz, $CDCl_3$, ppm): 1.39 (4H, m), 1.66 (2H, m), 1.72 (2H, m), 2.45 (3H, s), 2.62 (6H, s), 4.02 (2H, t, J = 6.3 Hz), 4.29 (2H, t, J = 6.3 Hz), 6.91 (2H, s), 6.93 (2H, d, J = 2.4 Hz), 6.97 (1H, s), 3.34 (2H, d, J = 7.8 Hz), 7.55 (2H, d, J = 2.4 Hz), 7.77 (2H, d, J = 8.3 Hz), 8.07 (2H, d, J = 8.8 Hz).

2.3.3. Synthesis of 6-tosylhexyl 3,5-bis(4-amino-3-methylphenoxy) benzoate (**5**)

Pt/C powder (5.0%, 0.369 g) were dispersed in a solution of **4** (3.21 g, 4.73 mmol) in 24 ml of THF and 23 ml of ethanol. The mixture was degassed under reduced pressure at −78 °C, and the reaction vessel was purged with hydrogen over 101 kPa. Then, the mixture was stirred at room temperature for 64 h. After Pt/C was filtered off washing with THF, the product was purified by column chromatography on silica gel with ethyl acetate/hexane (1/1 v/v) to obtain 1.44 g of **5** as a brown viscous liquid (Yield: 49.1%).

^{1}H NMR: δ (500 MHz, $CDCl_3$, ppm): 1.19 (4H, m), 1.52 (4H, m), 2.05 (6H, s) 2.39 (3H, s), 4.00 (2H, t, J = 12.5 Hz), 4.11 (2H, t, J = 13.0 Hz), 6.63 (1H, s), 6.66 (1H, s), 6.67 (1H, t, J = 2.5 Hz), 6.68 (1H, d, J = 2.5 Hz), 6.69 (1H, d, J = 2.5 Hz), 6.74 (2H, d, J = 2.5 Hz), 6.94 (2H, d, J = 2.0 Hz), 7.45 (2H, d, J = 8.0 Hz), 7.77 (2H, d, J = 8.5 Hz).

IR, ν (KBr, cm^{-1}): 3460 (-NH_2), 3381, 2936 (C-H), 1715 (C=O), 1597 (C=C), 1499, 1439, 1418, 1385, 1306, 1225, 1161 (S=O), 1119 (C-O-C), 1097, 1015, 961, 926, 816, 758.

2.3.4. Synthesis of 3-{3,5-bis(4-amino-3-methylphenoxy) benzoyloxyhexyl}-1- methylimidazolium tosylate (**DA-ImC1**)

The compound **5** (3.75 g, 6.07 mmol) was mixed with 1-methylimidazole (2.49 g, 30.4 mmol), and the mixture was stirred at 65 °C for 12 h. Then, a small amount of acetone was added, and excess hexane was poured into the solution. The precipitate was separated by decantation and dried *in vacuo* to obtain 3.18 g of **DA-ImC1** as a purple viscous liquid (Yield: 74.8%).

^{1}H NMR: δ (500 MHz, DMSO-d_6, ppm): 1.23 (2H, m), 1.32 (2H, m), 1.60 (2H, m), 1.75 (2H, m), 2.07 (6H, s), 2.28 (3H, s), 3.82 (3H, s), 4.13 (2H, t, J = 7.3 Hz), 4.18 (2H, t, J = 5.3 Hz), 6.67 (1H, t, J = 2.3 Hz), 6.71 (3H, s), 6.77 (2H, s), 6.98 (2H, d, J = 1.0 Hz), 7.10 (2H, d, J = 8.0 Hz), 7.46 (2H, d, J = 8.0 Hz), 7.68 (1H, s), 7.74 (1H, s), 9.08 (1H, s).

IR, ν (KBr, cm^{-1}): 3359 (-NH_2), 2939 (C-H), 1712 (C=O), 1595 (C=C), 1500, 1438, 1305, 1163 (S=O), 1122 (C-O-C), 1033, 1012, 817, 756.

2.3.5. Synthesis of 1-tosyl-9-methyltri(ethylene glycol)

Under an argon atmosphere, triethylene glycol monomethyl ether (12.4 g, 75.5 mmol) and triethylamine (17.7 ml, 126 mmol) were dissolved in 10 ml of dry THF. Then, the solution of tosyl chloride (12.1 g, 62.9 mmol) dissolved in 5 ml of dry THF was added dropwise at 0 °C, and the mixture was stirred at room temperature for 18 h. After the mixture was poured into excess water, the organic product was extracted with chloroform, and purified by column chromatography on silica gel with ethyl acetate/hexane (1/1 v/v) to obtain 17.9 g of 1-tosyl-9-methyltri(ethylene glycol) as a pale yellow liquid (Yield: 88.8%).

^{1}H NMR: δ (500 MHz, $CDCl_3$, ppm): 2.45 (3H, s), 3.37 (3H, s), 3.53 (2H, m), 3.59 (6H, m), 3.68 (2H, t, J = 5.0 Hz), 4.16 (2H, t, J = 5.0 Hz), 7.33 (2H, d, J = 8.0 Hz), 7.79 (2H, d, J = 8.5 Hz).

2.3.6. Synthesis of 1-{9-methyltri(oxyethylenyl)}imidazole (**6**)

To a solution of 1-tosyl-9-methyltri(ethylene glycol) (8.01 g, 25.2 mmol) and imidazole (2.14 g, 31.5 mmol) dissolved in 34 ml of THF, 4 ml of aqueous solution containing NaOH (1.00 g, 25.2 mmol) were added, and the mixture was refluxed for 6 h. After the mixture was poured into excess water, the organic products were extracted with chloroform, and purified by column chromatography on silica gel with chloroform/methanol (9/1 v/v) to obtain 3.20 g of **6** as a pale yellow liquid (Yield: 59.3%).

^{1}H NMR: δ (500 MHz, $CDCl_3$, ppm): 3.38 (3H, s), 3.53–3.55 (2H, m), 3.61–3.62 (6H, m), 3.75 (2H, t, J = 5.0 Hz), 4.13 (2H, t, J = 5.3 Hz), 7.01 (1H, s), 7.06 (1H, s), 7.63 (1H, s).

2.3.7. Synthesis of 3-{3,5-bis(4-amino-3-methylphenoxy) benzoyloxyhexyl}-1- {9-methyltri(oxyethylenyl)}imidazolium tosylate (**DA-ImEO**)

The compound **5** (1.44 g, 2.33 mmol) and the compound **6** (1.99 g, 9.32 mmol) were mixed in a flask, and the mixture was stirred at 50 °C for 7 h. After the mixture was washed with ethyl acetate, the precipitate was separated by decantation and dried *in vacuo* to obtain 1.10 g of **DA-ImEO** as a brown viscous liquid (Yield: 56.7%).

^{1}H NMR: δ (500 MHz, DMSO-d_6, ppm): 1.24 (2H, m), 1.33 (2H, m), 1.60 (2H, m), 1.77 (2H, m), 2.06 (6H, s), 2.29 (3H, s), 3.22 (3H, s), 3.40 (2H, m), 3.47 (4H, m), 3.53 (2H, m), 3.76 (2H, t, J = 5.0 Hz), 4.18 (4H, m), 4.34 (2H, t, J = 5.0 Hz), 6.64–6.67 (5H, m), 6.74 (2H, d, J = 2.0 Hz), 6.96 (2H, d, J = 2.0 Hz), 7.11 (2H, d, J = 8.0 Hz), 7.47 (2H, d, J = 8.0 Hz), 7.75 (1H, s), 7.79 (1H, s), 9.11 (1H, s).

IR, ν (KBr, cm^{-1}): 3465 (-NH_2), 2900, 2866 (C-H), 1716 (C=O), 1595 (C=C), 1500, 1436, 1303, 1191, 1161, 1122 (C-O-C), 1012, 815, 796.

2.4. Preparations of polymers containing imidazolium groups

2.4.1. Preparation of ***PI-ImC1***

Under an argon atmosphere, a solution of ODPA (0.872 g, 2.81 mmol) dissolved in 8.0 ml of anhydrous DMAc was added dropwise to a solution of **DA-ImC1** (1.97 g, 2.81 mmol) dissolved in 9.0 ml of DMAc. After the mixture was stirred at room temperature for 20 h, 1.64 ml of acetic anhydride and 3.13 ml of triethylamine were added, and the mixture was stirred at 80 °C for 5 h. Then, the reaction mixture was poured into excess methanol to produce a brown precipitate, and the product was purified by the reprecipitation from its DMAc solution to excess methanol. Finally, the product was dried *in vacuo* to afford 1.86 g of **PI-ImC1** as a brown powder (Yield: 68.4%).

^{1}H NMR: δ (500 MHz, DMSO-d_6, ppm): 1.28 (2H, m), 1.39 (2H, m), 1.69 (2H, m), 1.79 (2H, m), 2.15 (6H, s), 2.29 (3H, s), 3.82 (3H, s), 4.14 (2H, m), 4.25 (2H, m), 7.10 (2H, d, J = 8.0 Hz), 7.18 (2H, s), 7.34 (2H, s), 7.42 (2H, 3), 7.48 (2H, d, J = 8.0 Hz), 7.65–7.68 (4H, m), 7.75 (1H, s), 8.08 (2H, m), 9.09 (1H, s).

IR, ν (KBr, cm^{-1}): 2928, 2860, 1719 (C=O), 1600 (C=C), 1578, 1375, 1167 (S=O), 1242 (C-O-C), 1101.

2.4.2. Preparation of ***PIF-ImC1***

Under an argon atmosphere, a solution of 6FDA (0.80 g, 1.90 mmol) dissolved in 6.1 ml of anhydrous DMAc was added dropwise to a solution of **DA-ImC1** (1.30 g, 1.90 mmol) dissolved in 7.0 ml of DMAc. After the mixture was stirred at room temperature for 19 h, 1.4 ml of acetic anhydride and 2.1 ml of triethylamine were added, and the mixture was stirred at 80 °C for 5 h. Then, the reaction mixture was poured into excess methanol to produce a brown precipitate, and the product was purified by the reprecipitation from its DMAc solution to excess ethyl acetate. Finally, the product was dried *in vacuo* to afford 1.90 g of **PIF-ImC1** as a brown powder (Yield: 88.4%).

^{1}H NMR: δ (500 MHz, DMSO-d_6, ppm): 1.22 (3H, m), 1.36 (2H, m), 1.66 (2H, m), 1.76 (2H, m), 2.15 (5H, s), 2.29 (3H, s), 3.82 (3H, s), 4.14 (3H, t, J = 7.0 Hz), 4.25 (3H, m), 7.08 (1H, m), 7.12 (2H, d, J = 8.0 Hz), 7.18 (2H, m), 7.34 (2H, m), 7.44 (1H, m), 7.46 (2H, d, J = 8.0 Hz), 7.68 (4H, s), 7.74 (1H, s), 7.83 (2H, m), 7.94 (2H, m), 8.17 (2H, d, J = 8.0 Hz), 9.1 (1H, s).

IR, ν (KBr, cm^{-1}): 3082, 2934, 2864, 1732 (C=O), 1582 (C=C), 1499, 1441, 1416, 1377, 1302, 1244 (C-O-C), 1209, 1192, 1167 (S=O), 1105, 723, 681.

2.4.3. Preparation of ***PA-ImC1***

Under an argon atmosphere, a solution of terephthaloyl chloride (0.50 g, 1.70 mmol) dissolved in 4.3 ml of anhydrous *N*-methylpyrrolidone (NMP) was added dropwise at −78 °C to a solution of **DA-ImC1** (1.19 g, 1.70 mmol) dissolved in 5.0 ml of NMP. After the mixture was stirred at room temperature for 20 h, the reaction mixture was poured into excess THF to produce a brown precipitate, and the product was purified by the reprecipitation from its NMP solution to excess THF. Finally, the product was dried *in vacuo* to afford 1.10 g of **PI-ImC1** as a brown powder (Yield: 70.5%).

^{1}H NMR: δ (500 MHz, DMSO-d_6, ppm): 1.27 (3H, m), 1.34 (3H, m), 1.65 (3H, m), 1.75 (4H, m), 2.25 (5H, s), 2.28 (3H, s), 3.83 (4H, s), 4.13 (4H, t, J = 6.8 Hz), 4.21 (2H, m), 7.01 (2H, m), 7.11 (3H, d, J = 8.0 Hz), 7.23 (5H, d, J = 7.0 Hz), 7.39 (2H, m), 7.47 (2H, d, J = 8.5 Hz), 7.68 (1H, s), 7.75 (1H, s), 8.07 (4H, d, J = 5.0 Hz), 9.08 (1H, s), 9.92 (2H, m).

IR, ν (KBr, cm^{-1}): 2934, 2858, 1717 (C=O), 1655, 1595 (C=C), 1497, 1439, 1412, 1387, 1306, 1242 (C-O-C), 1205, 1163 (S=O), 1119, 1103, 872, 764.

2.4.4. Preparation of ***PI-ImEO***

Under an argon atmosphere, a solution of ODPA (0.200 g, 0.645 mmol) dissolved in 3.0 ml of anhydrous DMAc was added dropwise to a solution of **DA-ImEO** (0.537 g, 0.645 mmol) dissolved in 1.5 ml of DMAc. After the mixture was stirred at room temperature for 14 h, 0.48 ml of acetic anhydride and 0.72 ml of triethylamine were added, and the mixture was stirred at 80 °C for 5 h. Then, the reaction mixture was poured into excess ethyl acetate to produce a brown precipitate, and the product was purified by the reprecipitation from its DMAc solution to excess ethyl acetate. Finally, the product was dried *in vacuo* to afford 0.417 g of **PI-ImEO** as a brown powder (Yield: 58.4%).

^{1}H NMR: δ (500 MHz, DMSO-d_6, ppm): 1.28 (2H, m), 1.39 (2H, m), 1.69 (2H, m), 1.80 (2H, m), 2.15 (6H, s), 2.29 (3H, s), 3.21 (3H, s), 3.40 (2H, m), 3.47 (4H, m), 3.53 (2H, m), 3.76 (2H, t, J = 4.8 Hz), 4.17 (2H, t, J = 7.0 Hz), 4.26 (2H, s), 4.33 (2H, t, J = 4.8 Hz), 7.01 (1H, m), 7.10 (2H, d, J = 7.5 Hz), 7.19 (3H, s), 7.34 (2H, m), 7.42 (2H, m), 7.46 (2H, d, J = 8.0 Hz), 7.65–7.68 (4H, m), 7.74 (1H, s), 7.77 (1H, s), 8.08 (2H, d, J = 8.5 Hz), 9.11 (1H, s).

IR, ν (KBr, cm^{-1}): 3058, 2866, 1720 (C=O), 1600 (C=C), 1510, 1247 (C-O-C), 1162 (S=O), 750, 681.

2.4.5. Anion-exchange reaction of PI-ImEO with Li^+TFSI^- to prepare ***PI-ImEO(TFSI)***

Lithium bis(trifluoromethylsulfonyl)imide (Li^+TFSI^-, 0.150 g, 0.518 mmol) was added to a solution of PI-ImEO (0.287 g, 0.259 mmol) dissolved in 2.6 ml of dimethylformamide (DMF), and the mixture was stirred at 40 °C for 21 h to produce a brown precipitate. Then, the precipitate was filtered and dissolved again in 1.0 ml of DMF, and the solution was poured into excess methanol. The product was dried *in vacuo* to afford 0.257 g of **PI-ImEO(TFSI)** as a brown powder (Yield: 84.4%, Anion-exchange ratio: 90.8%).

^{1}H NMR: δ (500 MHz, DMSO-d_6, ppm): 1.25 (2H, m), 1.38 (2H, m), 1.68 (2H, m), 1.78 (2H, m), 1.80 (2H, m), 2.14 (6H, s), 2.29 (0.3H, s), 3.21 (3H, s), 3.44 (3H, m), 3.47 (3H, m), 3.53 (2H, m), 3.76 (2H, t, J = 4.0 Hz), 4.17 (2H, t, J = 6.5 Hz), 4.26 (2H, m), 4.33 (2H, t, J = 4.0 Hz), 7.10 (2H, m), 7.12 (0.4H, d, J = 8.0 Hz), 7.19 (3H, m), 7.34 (2H, m), 7.44 (2H, m), 7.48 (0.5H, d, J = 8.5 Hz), 7.66 (3H, m), 7.75 (1H, s), 7.78 (1H, s), 8.08 (2H, d, J = 7.5 Hz), 9.12 (1H, s).

IR, ν (KBr, cm^{-1}): 2860, 1719 (C=O), 1602 (C=C), 1500, 1350, 1248 (C-O-C), 1190 (C-F), 618.

2.5. Preparation of reference polyimide (PI)

2.5.1. Synthesis of 3,5-bis(4-nitro-3-methylphenoxy)benzene

5-Fluoro-2-nitrotoluene (24.2 g 156 mmol) and 1,3-dihydroxybenzene (7.80 g, 71.0 mmol) were dissolved in 227 ml of DMAc, and K_2CO_3 (19.6 g, 142 mmol) was added. After the mixture was stirred at 90 °C for overnight, the reaction mixture was poured into excess water, and the organic products were extracted with ethyl acetate. Then, the product was purified by recrystallization in acetone to obtain 18.1 g of 3,5-bis(4-nitro-3-methylphenoxy)benzene as a pale yellow solid (Yield: 67.1%).

^{1}H NMR: δ (500 MHz, DMSO-d_6, ppm): 2.04 (6H, s), 6.99 (1H, t, J = 2.25 Hz), 7.03 (1H, d, J = 3.00 Hz), 7.05 (2H, t, J = 2.25 Hz), 7.06 (1H, d, J = 2.00 Hz), 7.16 (2H, d, J = 2.50 Hz), 7.56 (1H, t, J = 8.25 Hz), 8.08 (2H, d, J = 9.50 Hz).

2.5.2. Synthesis of 3,5-bis(4-amino-3-methylphenoxy)benzene

Pt/C powder (5.0%, 0.500 g) were dispersed in a solution of 3,5-bis(4-nitro-3-methylphenoxy)benzene (3.10 g, 8.20 mmol) in 41 ml of THF. The mixture was degassed under reduced pressure at −78 °C, and the reaction vessel was purged with hydrogen over 101 kPa. Then, the mixture was stirred at room temperature for 24 h. After Pt/C was filtered off washing with THF, the product was

purified by column chromatography on silica gel with ethyl acetate/hexane (3/4 v/v) to obtain 2.10 g of 3,5-bis(4-amino-3-methylphenoxy)benzene as a brown powder (Yield: 81.1%).

^{1}H NMR: δ (500 MHz, DMSO-d_6, ppm): 2.04 (6H, s), 4.76 (4H, s), 6.33 (1H, t, J = 2.35 Hz), 6.42 (1H, d, J = 2.35 Hz), 6.45 (1H, d, J = 2.40 Hz), 6.60 (1H, s), 6.63 (2H, d, J = 2.50 Hz), 6.65 (1H, d, J = 2.50 Hz), 6.69 (2H, d, J = 2.50 Hz), 7.16 (1H, t, J = 8.25 Hz).

2.5.3. Preparation of PI

Under an argon atmosphere, a solution of ODPA (2.12 g, 6.70 mmol) dissolved in 12 ml of anhydrous DMAc was added dropwise to a solution of 3,5-bis(4-amino-3-methylphenoxy)benzene (2.06 g, 6.70 mmol) dissolved in 13 ml of DMAc. After the mixture was stirred at room temperature for 19 h, 5.00 ml of acetic anhydride and 7.4 ml of triethylamine were added, and the mixture was stirred at 80 °C for 5 h. Then, the reaction mixture was poured into excess methanol, and the product was purified by the reprecipitation from its DMAc solution to excess methanol. Finally, the product was dried *in vacuo* to afford 2.96 g of **PI** as a white powder (Yield: 75.0%).

^{1}H NMR: δ (500 MHz, DMSO-d_6, ppm): 2.11 (6H, s), 6.89 (2H, d, J = 8.00 Hz), 7.02 (2H, d, J = 8.00 Hz), 7.10 (2H, s), 7.38 (2H, d, J = 8.50 Hz), 7.47 (2H, t, J = 8.00 Hz), 7.64 (4H, s), 8.07 (2H, d, J = 9.00 Hz).

2.6. Characterization of monomers and polymers

^{1}H NMR spectroscopy was conducted with a BRUKER ADVANCE-500 NMR spectrometer (500 MHz), and the chemical shifts were estimated in ppm units with tetramethylsilane (TMS) as an internal standard. Infrared (IR) spectra were recorded with a Shimadzu FTIR-8400 spectrometer. Gel permeation chromatography (GPC) was carried out to determine the number-average (*M*n) and weight-average (*M*w) molecular weights with a Tosoh GPC system equipped with four columns of TSK gels, Multipore HXL-M, and RI detector of Tosoh RI-8010 with a pump of Tosoh CCPD using DMF solution containing 20 mM LiBr as an eluent at a flow rate of 1.0 ml min^{-1}. GPC was also conducted for THF-soluble polymers with a Tosoh HLC-8320GPC equipped with four columns of TSK gels, Super-Multipore HZ-H, using THF as an eluent at a flow rate of 1.0 ml min^{-1}. Standard polystyrenes were used to calibrate the molecular weights. Differential scanning calorimetry (DSC) and thermal gravimetric analysis (TGA) were carried out on Seiko Instruments DSC-6200 and TG/DTA-6200, respectively, at a heating rate of 10 °C min^{-1} under a nitrogen atmosphere.

2.7. Preparations of polymer membranes

Copolyimide membranes with a thickness of *ca.* 100 μm were prepared by solvent-casting method from the chloroform solutions on the polytetrafluoroethylene sheet and dried at 40 °C for 2 days. To complete the imidization, the thermal treatments of the obtained membranes were carried out at 180 °C for 24 h. Then, the film samples were cut into circular pieces with a diameter of 36 mm.

Polymer nanosheets were essentially fabricated using a method of Okamura et al. [37]. In order to produce a water-soluble sacrificial layer, an aqueous solution of sodium alginate (20 mg ml^{-1}) was dropped on a silicon oxide (SiO_2) substrate (KST World Co., Fukui, Japan) and then spin-coated at 4000 rpm for 20 s, followed by a drying step at 50 °C for 90 s. Following the same procedure, the sodium alginate-coated SiO_2 substrate was then coated with imidazolium-containing polymer solutions dissolved in NMP (30–100 mg ml^{-1}). The substrates were immersed in distilled water at room temperature to obtain free-standing nanosheets. Then, the obtained nanosheets (4 cm × 4 cm) were washed several times with distilled water to completely remove sodium alginate. Finally, each nanosheet was softly attached with PIS12 membrane (4 cm × 4 cm) on the surface of water to obtain the composite membrane of nanosheet/PIS12. The obtained composite membrane was dried at room temperature in desiccator followed by drying in vacuum oven at room temperature.

2.8. Characterizations of membranes

The measurements of thickness of nanosheets, which were pasted on SiO_2 substrates, were carried out using a microfigure measuring instrument ET200 (Kosaka Laboratory Ltd., Tokyo, Japan). The thickness of PIS12 membrane was determined using digimatic micrometer QuantuMike IP65 (Mitutoyo Corporation, Kanagawa, Japan).

Contact angle of water on the surface of the membrane was measured by sessile drop method using Kyowa DropMaster DMe-201 (Kyowa Interface Science Co., LTD., Saitama, Japan) at room temperature.

2.9. Measurement of adhesive strength of nanosheet

The adhesive strength of nanosheets was measured by a scratch tester for thin films (model CSR-2000, Rhesca Co., Tokyo, Japan). The procedure in brief was as follows: a diamond tip at a radius of curvature of 25 μm was continuously and vertically loaded at a rate of 20 mN/min, and used to horizontally scratch the polymer nanosheets readsorbed on the SiO_2 substrate (scratch length: 600 μm, scratch rate: 10 μm/s). The signal of frictional vibration just after detaching the nanosheet was detected (designated a critical load). Then, the critical loads of nanosheets were measured with changing thickness from 10 to 650 nm and corrected the critical loads divided by the thickness. The critical loads were measured in triplicate.

2.10. Measurements of gas permeability

Gas permeability coefficients of six kinds of pure gases, *i.e.* hydrogen, oxygen, nitrogen, carbon dioxide, methane and ethane, were measured by the ordinary vacuum method using Tsukuba-Rikaseiki K-315N-01 (Tsukuba-Rikaseiki Co. Ltd., Tokyo, Japan), where the permeation area was 7.07 × 10^{-4} m^2. The pressures of upstream and downstream sides were about 100 and 0.1 kPa, respectively, and the cell temperature was kept at 30 °C. The gas permeability coefficients (P, m^3 (STP) m m^{-2} s^{-1} Pa^{-1}) were computed from the slope of the time-pressure curve, dp/dt, in the steady state with following equation:

$$P = \frac{\mathrm{d}p}{\mathrm{d}t}\frac{V}{A}\frac{L}{p_0}\frac{273}{T} \quad (1)$$

where V is the volume of the downstream chamber (m^3), L is the membrane thickness (m). A is the effective test area of the membrane (m^2), p_o is the upstream operating pressure (Pa), and T is the operating temperature (K).

According to the Fick's law, the pure gas permeability (P) can be given by:

$$P = DS \quad (2)$$

where D is the diffusivity coefficient with the unit of m^2 s^{-1} and S is the sorption coefficient with the unit of m^3 (STP) m^{-3} Pa^{-1}. The diffusivity coefficient was calculated by the time-lag method as Equation (3), and then the solubility coefficient was simply

deduced according to Equation (2).

$$D = \frac{L^2}{6\theta} \quad (3)$$

Where θ is the diffusion time lag extrapolated from the plot of pressure with time at steady state to the time axis.

3. Results and discussion

3.1. Preparation of PIS12 as a material for the base membrane

In our previous study, we have developed novel PDMS graft copolyimide as a material for separation membrane, which has oligomeric PDMS side chains in every repeating units and shows the high gas and liquid permeability with excellent mechanical strength [37,38]. For the synthesis of PDMS graft copolyimide, the polycondensation of 3,5-bis(4-aminophenoxy)benzyloxypropyl-terminated PDMS macromonomer with 6FDA or 3,5-bis(4-amino-3-methylphenoxy)benzyloxypropyl-terminated PDMS macromonomer with ODPA was carried out followed by chemical imidization to obtain soluble copolyimide [37], which gave tough films easily by solvent-casting method. However, 3,5-dihydroxybenzyl chloride, the starting compound for the synthesis of PDMS macromonomer, was an expensive reagent. Therefore, we attempted to improve the molecular design of diamino-terminated PDMS macromonomer using the cheaper reagent, methyl 3,5-dihydroxybenzoate, as the starting compound, where PDMS chain was connected with diamine moiety via ester linkage.

The synthetic procedures of PDMS macromonomer (**3**) and PDMS graft copolyimide (**PIS12**) are shown in Scheme 1. The starting compound, 3,5-bis(4-nitro-3-methylphenoxy)benzoic acid (BNMPB), was prepared by etherification of methyl 3,5-hydroxybenzoate with 5-fluoro-2-nitrotoluene followed by hydrolysis of the methyl ester moiety [40]. Then, dinitro-terminated PDMS (**2**) was prepared by hydrosilylation of 3-butenyl ester of BNMPB (**1**) with hydrosilyl-terminated PDMS, and the hydrogen reduction of **2** gave the macromonomer (**3**). In this synthetic route, if allyl ester of BNMPB was used for the hydrosilylation instead of **1**, the product yield was very low (less than 20%) because the chain scission of ester linkage occurred to produce BNMPB [40]. It would be due to the effect of silyl group connected to the ester linkage with propylene spacer. Thus, by using 3-butenyl ester of BNMPB (**1**), the hydrosilylation proceeded smoothly to obtain **2** in the better yield (74%).

On the other hand, as a dianhydride monomer for the synthesis of polyimide, 6FDA is a very expensive as compared with ODPA, although 6FDA is a useful monomer to afford a soluble polyimide. The methyl groups connected to the next position of amino groups of the terminal group of macromonomer **3** plays an important role to make the obtained polyimide soluble in several solvents, even if ODPA is used as a dianhydride monomer [35]. Consequently, as the material for base membrane, PDMS graft copolyimide was prepared by polycondensation of PDMS macromonomer **3** with ODPA followed by chemical imidization with acetic anhydride (Ac_2O) and triethylamine as shown in Scheme 1. ^{1}H NMR spectra of **3** and **PIS12** are added in supporting information as Figs. S1 and S2, respectively. The obtained polyimide, **PIS12**, was soluble in THF, chloroform and aprotic polar solvents such as DMF, DMAc, dimethylsulfoxide (DMSO) and NMP, as we expected. The molecular weights of **PIS12** are listed in Table 1. The degree of polymerization of PDMS segment of **PIS12** was fixed at 12–13, which would be a suitable length to exhibit the high gas permeability coefficients as the same order as PDMS cross-linked membrane and also the good mechanical strength [36]. The tough self-standing membranes could be prepared by solvent-casting method from the chloroform solutions of **PIS12**, although the low *Tg* PDMS chains were included in every repeating units over the content of 55 wt.%.

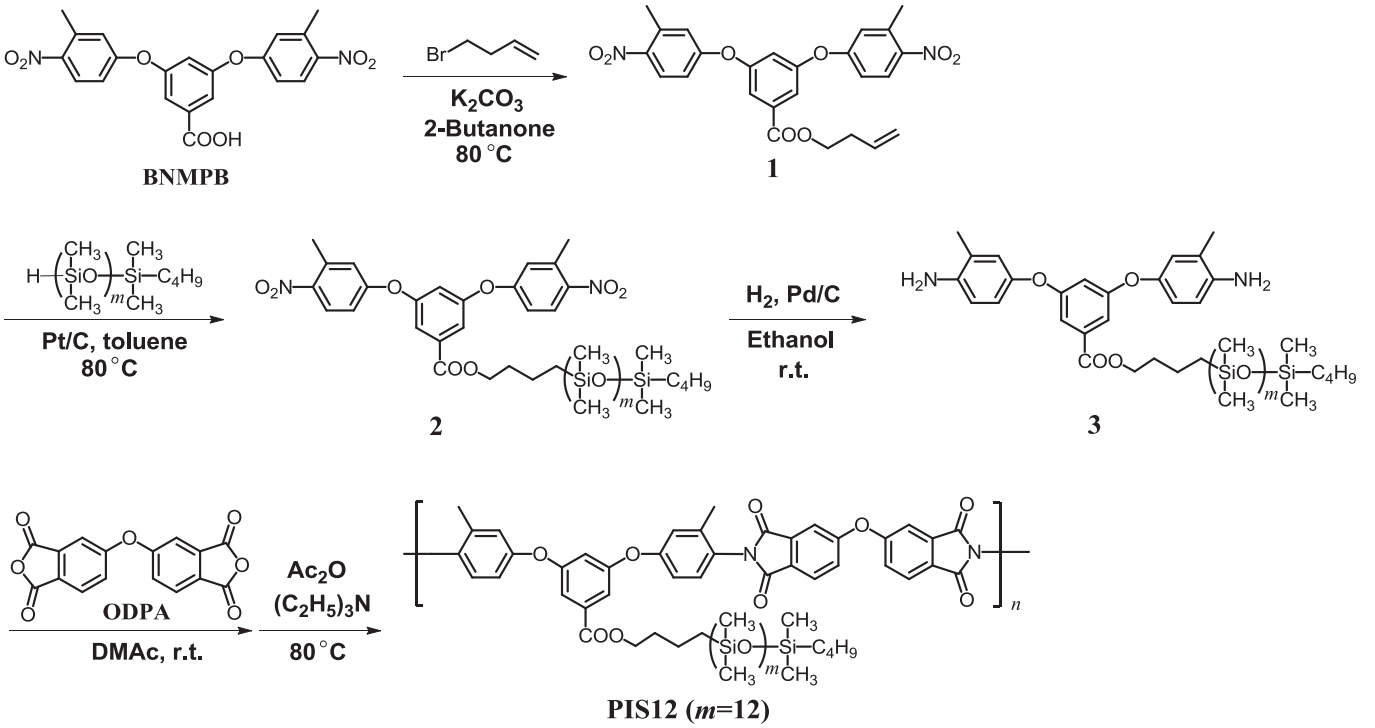

Scheme 1. Syntheses of diamino-terminated PDMS macromonomer and PDMS graft copolyimide (PIS12).

Table 1
Molecular weights and thermal properties of the obtained polymers.

Code	$Mn \times 10^{-3}$	$Mw \times 10^{-3}$	Mw/Mn	Tg (°C)[c]	T_{d5} (°°C)[d]
PIS12	29.5[a]	52.3[a]	1.77[a]	−102[e]	370
PI-ImC1	8.86[b]	10.9[b]	1.23[b]	150	347
PI-ImEO	20.0[b]	86.0[b]	4.30[b]	59	338
PIF-ImC1	11.9[b]	17.5[b]	1.47[b]	–[f]	333
PA-ImC1	16.0[b]	23.9[b]	1.49[b]	120	328
PI-ImEO(TFSI)	–	–	–	62	358
PI	25.1[a]	37.8[a]	1.51[a]	211	507

[a] Number- and weight-average molecular weights (*Mn* and *Mw*) were determined by GPC using THF as an eluent.
[b] Number- and weight-average molecular weights (*Mn* and *Mw*) were determined by GPC using DMF solution containing 2.0 M LiBr as an eluent.
[c] Glass transition temperature (*Tg*) was determined by DSC at a heating rate 10 °C/min on the 2nd heating scan in N_2 flow.
[d] Temperature at 5% weight loss (T_{d5}) was determined by TGA at a heating rate 10 °C/min on the 2nd heating scan in N_2 flow.
[e] *Tg* of PDMS segments was detected at −102 °C, but the higher *Tg* was not detected up to 300 °C.
[f] *Tg* was not detected in DSC curves between −50 °C and 200 °C.

3.2. Preparations of imidazolium-containing polymers as a surface layer

According to the similar strategy as PDMS macromonomer, dimethyl-substituted diamine monomers containing imidazolium groups were designed and synthesized as shown in Scheme 2. The compound **4** is a key intermediate to introduce imidazolium group with tosylate anion and to afford diamine monomers by a reduction of the two nitro groups. At first, we attempted to prepare the monomer, **DA-ImC1**, by the reaction of **4** with 1-methylimidazole followed by the hydrogen reduction of dinitro groups. However, the hydrogen reduction of the imidazolium compound did not completely proceed to obtain a lot of byproducts. Therefore, the hydrogen reduction of **4** was carried out at first to obtain the diamine compound **5**, and then the quaternization of **5** with 1-methylimidazole proceeded successfully to obtain the desired monomer, **DA-ImC1**, in good yield. Furthermore, another imidazolium-containing monomer with oligo(ethylene oxide) chain, **DA-ImEO**, was also prepared from compound **6** instead of 1-methylimidazole according to the same procedure as the case of **DA-ImC1**. It was reported that such a combination of imidazolium group and oligo(ethylene oxide) chain was effective to exhibit the high CO_2 permselectivity of polyimide membranes [26]. ^{1}H NMR spectra of **DA-ImC1** and **DA-ImEO** are added in supporting information as Figs. S3 and S4, respectively.

From these two diamine monomers, three kinds of polyimides, **PI-ImC1**, **PIF-ImC1** and **PI-ImEO**, and an aromatic polyamide, **PA-ImC1**, were prepared as shown in Scheme 3, to investigate the effect of backbone structure on the gas permselectivity. All of the polymers were soluble in aprotic polar solvents, such as DMF, DMAc, DMSO and NMP, but insoluble in THF and chloroform. Therefore, the introduction of methyl groups in the diamine monomers would be effective to obtain soluble polyimide, even though ODPA was used as an acid anhydride monomer. ^{1}H NMR spectra of these polymers are added in supporting information as Figs. S5–S8.

Bara et al. have investigated the effect of counter anion on the gas separation performance of ionic liquid composite membranes, and reported that bis(trifluoromethylsulfonyl)imide anion ($TFSI^-$) was effective to increase the permeability of CO_2 without decreasing the good selectivity of CO_2/N_2 and CO_2/CH_4 [22]. Therefore, we attempted to exchange the counter anion of these polymers to $TFSI^-$ from tosylate anion (Tso^-). As a result, unfortunately, the anion exchange reaction of **PI-ImC1** with Li^+TFSI^- gave an insoluble polymer. On the contrary, we succeeded to obtain a soluble polymer by exchanging the anion of PI-ImEO using Li^+TFSI^- to afford **PI-ImEO(TFSI)** as shown in Scheme 3. The solubility of **PI-ImEO(TFSI)** was almost same as that of **PI-ImEO**, which would be due to the flexible oligo(ethylene oxide) side chain. ^{1}H NMR spectrum of **PI-ImEO(TFSI)** is added in supporting information as Fig. S9.

On the other hand, a normal polyimide without imidazolium group (**PI**) was synthesized by the similar procedure of **PI-ImC1** using 3,5-bis(4-amino-3-methylphenoxy)benzene and ODPA as monomers. The solubility of **PI** was similar to **PIS12**.

The molecular weights and the thermal properties of the

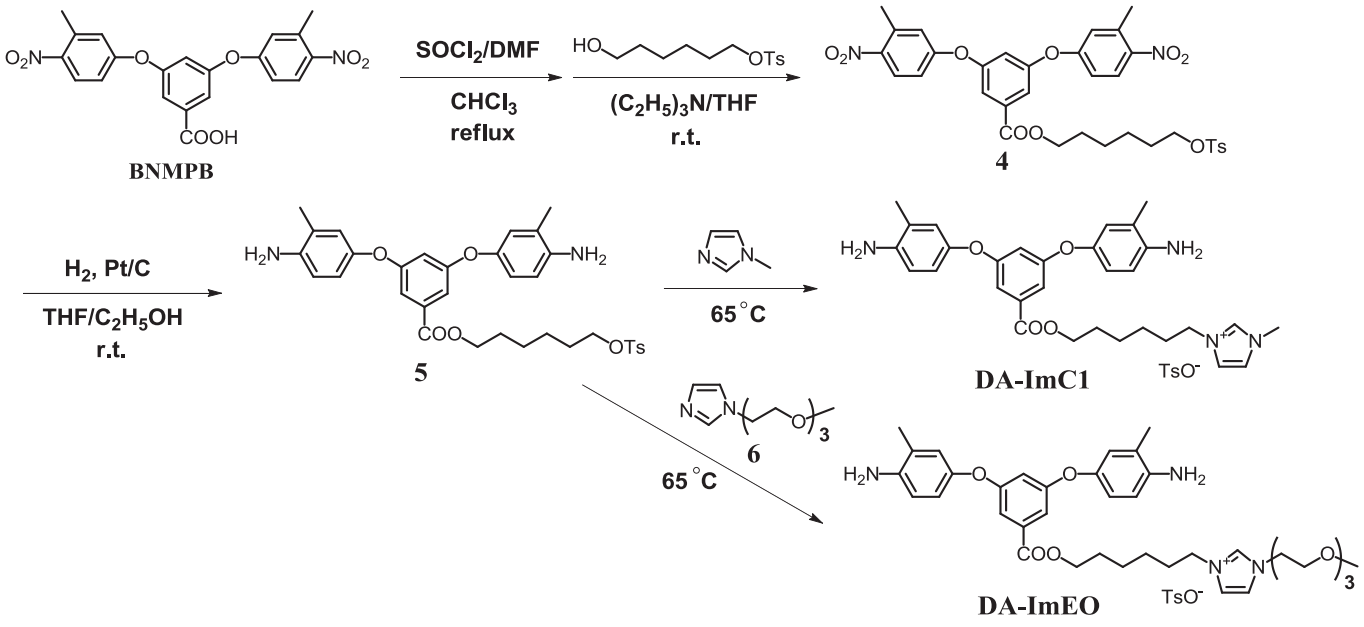

Scheme 2. Syntheses of diamine monomers containing imidazolium moiety with tosylate anion.

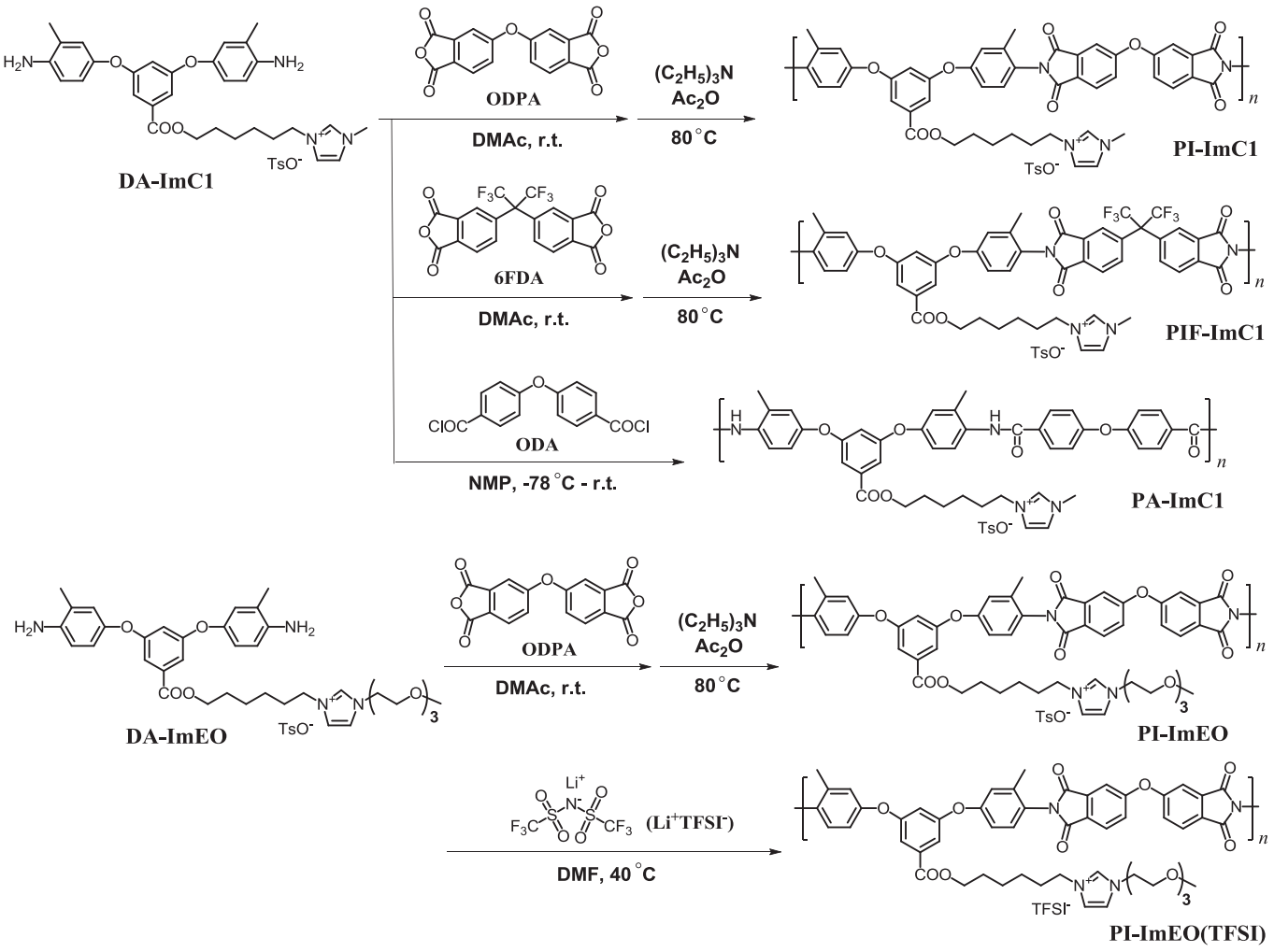

Scheme 3. Polymerizations of diamine monomers containing imidazolium moiety and the anion-exchange reaction.

obtained polymers are summarized in Table 1. The gel permeation chromatography (GPC) measurement of **PI-ImEO(TFSI)** could not be conducted because it was only partially soluble in DMF and insoluble in THF. Based on the GPC results, the weight-average molecular weights of **PI-ImC1**, **PIF-ImC1**, **PI-ImEO**, **PA-ImC1** and **PI** were in the order of 10^4. Unfortunately, self-standing films of these polymers could not be obtained by solvent casting method because of their brittle properties, but nanosheets of these polymers successfully prepared as described in the next section.

The glass transition temperatures (T_g) of **PI-ImC1** and **PA-ImC1** were detected at 150 °C and 100 °C, respectively, by the measurements of DSC. On the contrary, after the incorporation of flexible oligo(ethylene oxide) chains, the obtained polyimides, **PI-ImEO** and **PI-ImEO(TFSI)**, have undergone an enormous decrease in T_g. According to TGA, thermal degradation temperatures (T_{d5}, the temperature at 5% weight loss) of these polymers were estimated up to 300 °C as shown in Table 1. The decompositions of ionic imidazolium groups would be a trigger of the thermal degradations, because T_{d5} of PI was observed over 500 °C. DSC and TGA curves of these polymers are shown in supporting information as Figs. S10 and S11.

3.3. Preparations of composite membranes

We attempted to prepare ultra-thin films, so called nanosheets, from imidazolium-containing aromatic polymers by the procedure reported by Okamura et al. [39]. The fabrication of a polymer nanosheet is illustrated in Fig. 1(A). Sodium alginate (Na-Alg) was used as a water-soluble sacrificial layer, and a polymer solution dissolved in NMP and DMSO was cast on the substrate previously spin-coated with aqueous Na-Alg solution and dried. Then, the double layered substrate was immersed in water to obtain easily a self-standing nanosheet after Na-Alg was dissolved in water. The macroscopic image of the obtained nanosheet of PI-ImC1 is shown in Fig. 1(B), where the nanosheet floated on the surface of water. The resulting films were flexible and transparent. In this procedure, the thickness of the obtained nanosheets could be controlled by changing the concentration of polymer solution, as shown in Fig. 2. The relationships between the polymer concentrations and the thicknesses of the nanosheets were different in each polymer, which would be due to the difference of viscosities of the polymer solutions.

On the other hand, we estimated the adhesive strength of PI-ImC1 nanosheets attached on SiO_2 substrate using a scratch tester for thin films. When the thickness was below 100 nm, the adhesion strength was significantly increased. It was considered that the nanosheets with a large contact area could conform to the substrate surface because of its flexibility and low roughness as describes in the literature [39]. The adhesive strengths of the nanosheets prepared from PI-ImC1 consisting of various thicknesses were in the

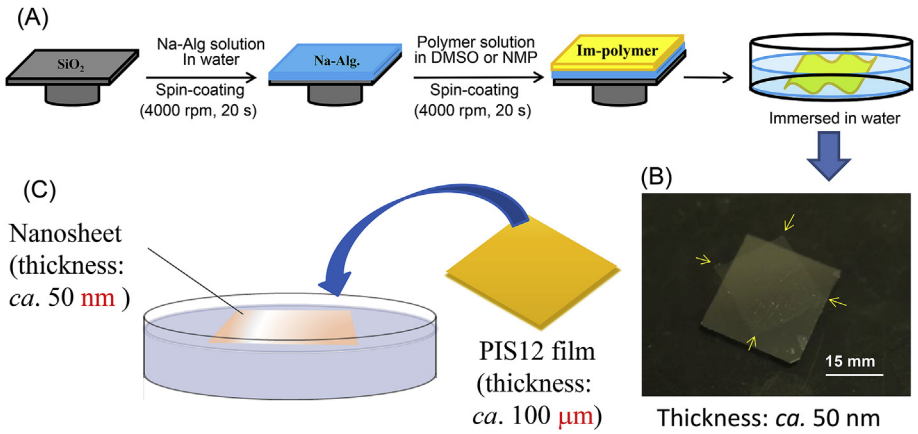

Fig. 1. (A) Schematic illustration for the fabrication of nanosheets, (B) a macroscopic image of the obtained nanosheet of PI-ImC1 and (C) an illustration for the fabrication of composite membrane.

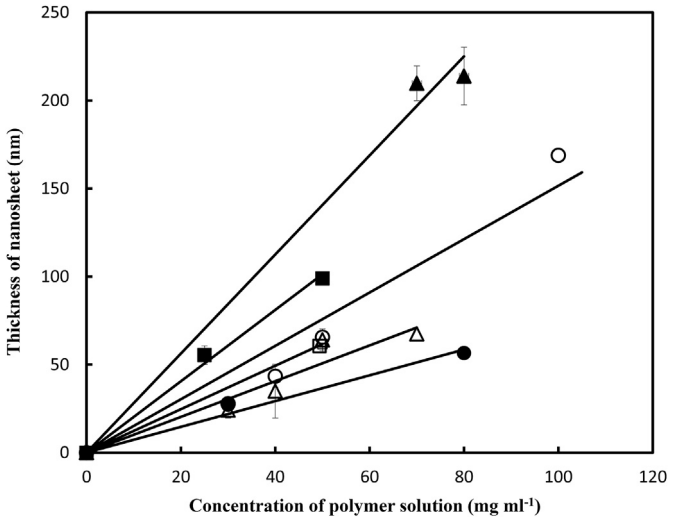

Fig. 2. Relationship between the concentration of polymer solutions for spin coating and the thickness of the nanosheets of PI-ImC1 (●), PI-ImEO (■), PIF-ImC1 (○), PA-ImC1 (△), PI-ImEO(TFSI) (□) and PI (△).

values of 10.9×10^3 N/m (thickness: 11.9 nm), 5.72×10^3 N/m (thickness: 27.4 nm), 1.39×10^3 N/m (thickness: 93.4 nm), 0.220×10^3 N/m (thickness: 640 nm), respectively. Consequently, the greatest benefit of the nano-thickness is the high potential to adhere on the substrate.

The attachments of the polymer nanosheet on **PIS12** cast membranes have been achieved easily on the surface of water, where the nanosheets were covered on the surface of **PIS12** membranes. As shown in Table 2, the water contact angles on the surface of all the composite membranes are lower than that of PIS12 base membrane. It was considered that the hydrophobic **PIS12** membranes covered with PDMS chains have become relatively hydrophilic by the nanosheet-coatings of these ionic polymers. Furthermore, according to the difference of main chain structures in these ionic polymers, the different surface hydrophilicities were observed. The coatings of **PIF-ImC1** and **PA-ImC1** resulted in the more hydrophobic surfaces as compared with the cases of **PI-ImC1** and **PI-ImEO**. The contact angles of **PIF-ImC1** and **PA-ImC1** were similar to that of **PI**. In the case of **PIF-ImC1**, the trifluoromethyl groups in the dianhydride monomer (6FDA) would increase the hydrophobicity of the nanosheet surface. On the contrary, polyimides containing polar oligo(ethylene oxide) as well as imidazolium group, **PI-ImEO** and **PI-ImEO(TFSI)**, exhibited the lowest contact angles of water, which should be associated with hydrophilic oligo(ethylene oxide) segment.

3.4. Gas permselectivity of the composite membranes

Gas permeability coefficients of **PIS12** and the composite membranes were evaluated for pure gases, *i.e.* H_2, O_2, N_2, CO_2, CH_4 and C_2H_6, by the ordinary vacuum method. The results are summarized in Table 3. The thicknesses of each layer of the composite membranes were the same as listed in Table 2. In the cases of **PIF-ImC1** and **PI**, as the thin nanosheet less than 100 nm thick could not be obtained in the large area of 4 cm × 4 cm, the thicknesses of **PIF-ImC1** and **PI** layers were 169 nm and 210 nm, respectively. For the other composite membranes, the thicknesses of the nanosheet layers were in the range of 55–68 nm on **PIS12** base membranes, the thickness of which were 106–137 μm.

As can be seen in Table 3, the gas permeability coefficients of the composite membranes for all gases except H_2 considerably decreased as compared with those of **PIS12** base membrane. This phenomenon would be attributed to the densification of **PIS12**

Table 2
The contact angle of water on the surface of PIS12 and composite membranes.

Code	Thickness of each layer (nm/μm)	Contact angle of water (degree)
PIS12	0/132	100.0 ± 1.0
PI-ImC1/PIS12	53/106	58.6 ± 1.3
PI-ImEO/PIS12	55/113	52.5 ± 2.7
PIF-ImC1/PIS12	169/137	81.1 ± 6.0
PA-ImC1/PIS12	68/135	81.2 ± 4.9
PI-ImEO(TFSI)/PIS12	62/118	49.7 ± 3.9
PI/PIS 12	210/118	79.3 ± 2.6

Table 3
Gas permeability coefficients and separation factors of PIS12 and composite membranes at 30 °C.

Code	Gas permeability coefficient, P (Barrer[a])						Selectivity, P/PN_2				
	H_2	N_2	O_2	CO_2	CH_4	C_2H_6	H_2/N_2	O_2/N_2	CO_2/N_2	CH_4/N_2	C_2H_6/N_2
PIS12	243	90.8	201	1070	291	805	2.58	2.21	11.8	3.20	8.87
PI-ImC1/PIS12	201	6.97	44.1	218	6.80	9.43	28.8	6.33	31.3	0.976	1.35
PI-ImEO/PIS12	184	9.69	50.7	259	16.7	31.3	19.0	5.23	26.7	1.72	3.23
PIF-ImC1/PIS12	284	45.9	160	769	106	247	6.19	3.49	16.8	2.31	5.38
PA-ImC1/PIS12	263	14.3	64.5	258	28.7	64.2	18.4	4.51	18.1	2.01	4.49
PI-ImEO(TFSI)/PIS12	235	35.5	120	670	61.1	61.6	6.62	3.38	18.9	1.72	1.74
PI/PIS 12	263	32.5	124	564	66.8	150	8.09	3.82	17.4	2.05	4.62

[a] 1 Barrer = 7.52×10^{-15} m^3 (STP) m m^{-2} sec^{-1} Pa^{-1}.

surface by the polymer nanosheets, which acted as barrier layers according to these imidazolium polymers. Concerning the N_2 permeability coefficient, the layers of **PI-ImC1** and **PI-ImEO** exhibited the significant barrier properties, where PN_2 of the composite membranes considerably decreased as compared with **PIF-ImC1/PIS12**, **PA-ImC1/PIS12** and **PI/PIS12**. The similar tendency was observed in the CH_4 and C_2H_6 permeability coefficients, which were the permeations of hydrophobic gases through the hydrophilic ionic surface. On the other hand, PO_2 and PCO_2 of these composite membranes decreased not so much as compared with those of **PIS12** membrane. It would be due to the affinity of the surface layers against O_2 and CO_2 gases, although the layers acted as gas barrier. As a result, the selectivity of O_2/N_2 and CO_2/N_2 through **PI-ImC1/PIS12** and **PI-ImEO/PIS12** composite membranes significantly increased as compared with **PIS12** membrane.

The selectivity values of O_2/N_2 and CO_2/N_2 are plotted against the values of PO_2 and PCO_2, respectively, as shown in Fig. 3 compared with Robeson upper bound [39]. Although the tradeoff relation between the gas permeability and the selectivity was observed, **PI-ImC1/PIS12** composite membrane showed the best performance in the gas permselectivity, which were near to the upper bound of O_2/N_2. However, the surface layers of **PIF-ImC1**, **PA-ImC1** and **PI-ImEO(TFSI)** were not so effective to improve the selectivity of these gas pairs, where the permselectivities were similar to that of **PI** layer. It was considered that these polymer layers would have the relatively higher gas permeability than the layers of **PI-ImC1** and **PI-ImEO**. In fact, polyimides prepared from 6FDA have been known as relatively high gas permeable membrane materials. In addition, the anion exchange of **PI-ImEO** by $TFSI^-$ would decrease the density of the layer as described by Bara et al. [20].

The diffusion and solution coefficients of O_2, CO_2 and N_2 through PIS12, PI-ImC1/PIS12, PI-ImEO/PIS12, PIF-ImC1/PIS12 and PI/PIS12 membranes were estimated to investigate the difference of O_2/N_2 and CO_2/N_2 selectivity among these composite membranes, as shown in Table 4. The source values of the diffusion time lag (θ) for each gas are listed in supporting information as Table S1. The gas diffusion coefficients of the layered composite membranes actually decreased as compared with those of PIS12, which would be caused by the barrier property of surface layers. On the other hand, PI-ImC1/PIS12 and PI-ImEO/PIS12 composite membranes exhibited the higher values of solubility selectivity, SO_2/SN_2 and SCO_2/SN_2, than the other membranes. In addition, it was found that the diffusion coefficients, DO_2 and DCO_2, of these two composite membranes were the lower values than those of other three membranes. Therefore, it was considered that the surface layers composed of PI-ImC1 and PI-ImEO were effective to improve the O_2/N_2 and CO_2/N_2 selectivity owing to not only the relatively high

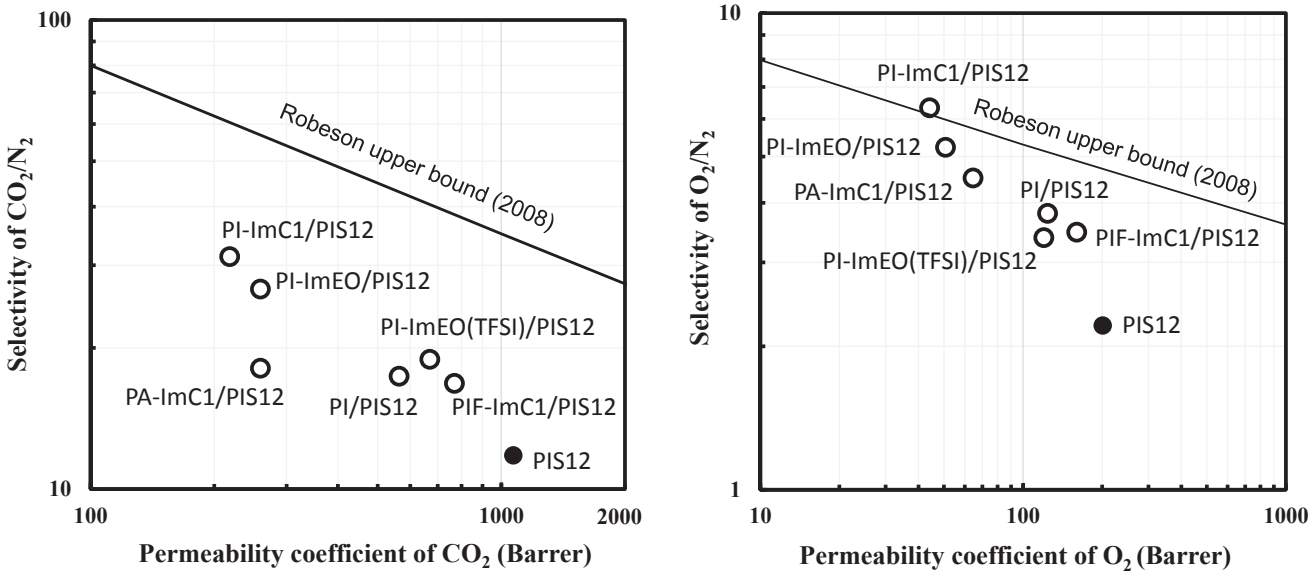

Fig. 3. Relationship between the permeability coefficients of O_2, CO_2 and the separation factors of O_2/N_2, CO_2/N_2 of PIS12 and the composite membranes with Robeson upper bound (2008) [41].

Table 4
The diffusion and solution coefficients of gas permeations through PIS12 and composite membranes at 30 °C.

Code	Diffusion coefficient, D (10^{-10} m^2 s^{-1})					Solution coefficient, S (10^{-3} m^3 (STP) m^{-3} Pa^{-1})				
	DO_2	DCO_2	DN_2	DO_2/DN_2	DCO_2/DN_2	SO_2	SCO_2	SN_2	SO_2/SN_2	SCO_2/SN_2
PIS12	8.43	5.20	7.73	1.09	0.672	1.76	14.7	0.873	2.01	16.8
PI-ImC1/PIS12	2.28	0.682	0.826	2.76	0.825	1.45	24.0	0.618	2.34	38.8
PI-ImEO/PIS12	3.84	1.74	2.58	1.48	0.674	0.992	11.1	0.281	3.51	39.3
PIF-ImC1/PIS12	6.53	4.18	2.63	2.48	1.58	1.84	13.8	1.31	1.40	10.5
PI/PIS12	11.9	3.28	5.94	2.00	0.552	0.783	12.9	0.411	1.90	31.3

solubility selectivity, SO_2/SN_2 and SCO_2/SN_2, but also the low diffusivity, DO_2 and DCO_2, in gas permeations.

3.5. Calculated gas permeability of nanosheet layers

To reveal the difference in gas permeability coefficients of these surface layers, we have calculated the gas permeability coefficients using the following equation (4):

$$\frac{l_0}{P_0} = \frac{l_1}{P_1} + \frac{l_2}{P_2} \tag{4}$$

where l_0 is a thickness of the composite membrane, l_1 is a thickness of **PIS12** base membrane, l_2 is a thickness of the surface layer, P_0 is a permeability coefficient of the composite membrane, P_1 is a permeability coefficient of **PIS12** base membrane, and P_2 is a permeability coefficient of the surface layer [42]. In this equation, l_0, l_1, l_2, P_1 and P_2 were measurable values, therefore, the permeability coefficient of each gas through surface layer, P_2, could be determined.

The calculated results for the permeability of N_2, O_2 and CO_2 are listed in Table 5. As we expected, the nanosheets layers of **PIF-ImC1**, **PI-ImEO(TFSI)** and **PI** exhibited the higher gas permeability than those of others. In addition, the selectivity of CO_2/N_2 through **PA-ImC1** layer showed relatively low value, which was similar to the case of **PI** layer. Therefore, it was found that the effective layers for the gas permselectivity, **PI-ImC1** and **PI-ImEO**, showed the low gas permeability and the relatively high selectivity. Consequently, concerning a suitable material for surface modification on the highly gas permeable membrane, the gas barrier property and the affinity for specific gas would play an important role to improve the selectivity of gases with maintaining the high gas permeability.

4. Conclusion

Aromatic polyimides and polyamide containing imidazolium moiety were successfully prepared from the novel ionic diamine monomers. From these polymers, we could fabricate the self-standing ultrathin films (nanosheets) with the thickness of 50–170 nm, and the surface modification of highly gas permeable membrane composed of **PIS12** was carried out using the obtained nanosheets. We are considering that this method of nanosheet-coating is useful for a surface modification of highly gas permeable membrane, because the solution-coating on the membrane would damage the membrane surface by organic solvents. It was found that such a nanosheet-coating by imidazolium-containing polymer was very effective to improve the selectivity of CO_2/N_2 and O_2/N_2, especially for the improvement of O_2/N_2, and the efficiency depended on the chemical structures of polymer backbone, imidazolium group and counter anion. Although it was our preliminary study for the surface modification by nanosheet-coating, the relatively dense surface layer would be more effective to enhance the gas separation property of the highly gas permeable membrane. From these points of view, we are now continuing to search the suitable surface layers to obtain the high gas permselective composite membranes.

Table 5
Calculated gas permeability coefficients and separation factors of nanosheet layers at 30 °C.

Code	Gas permeability coefficient, P (Barrer[a])			Selectivity, P/PN_2	
	N_2	O_2	CO_2	O_2/N_2	CO_2/N_2
PI-ImC1	3.77×10^{-3}	2.82×10^{-2}	13.7×10^{-2}	7.48	36.3
PI-ImEO	5.27×10^{-3}	3.29×10^{-2}	16.6×10^{-2}	6.25	31.5
PIF-ImC1	114×10^{-3}	96.1×10^{-2}	335×10^{-2}	8.42	29.4
PA-ImC1	8.54×10^{-3}	4.78×10^{-2}	17.2×10^{-2}	5.59	20.1
PI-ImEO(TFSI)	30.6×10^{-3}	15.6×10^{-2}	94.0×10^{-2}	5.11	30.7
PI	89.8×10^{-3}	57.3×10^{-2}	211×10^{-2}	6.38	23.5

[a] 1 Barrer = 7.52×10^{-15} m^3 (STP) m m^{-2} sec^{-1} Pa^{-1}.

Acknowledgment

This work was supported in part by the Ministry of Education, Culture, Sports, Science, and Technology of Japan (MEXT)-Supported Program for the Strategic Research Foundation at Private Universities. We express our sincere gratitude to Prof. Shinji Takeoka and Dr. Toshinori Fujie from the Department of Life Science and Medical Bioscience, School of Advanced Science and Engineering, Waseda University for their help in conducting the measurements of adhesive strength of nanosheets.

Appendix A. Supplementary data

Supplementary data related to this article can be found at https://doi.org/10.1016/j.polymer.2017.12.016.

References

[1] R.W. Baker, Ind. Eng. Chem. Res. 41 (2002) 1393–1411.
[2] M. Ulbricht, Polymer 47 (2006) 2217–2262.
[3] T. Aoki, T. Kaneko, M. Teraguchi, Polymer 47 (2006) 4867–4892.
[4] R.W. Baker, K. Lokhandwala, Ind. Eng. Chem. Res. 47 (2008) 2109–2121.
[5] P.M. Budd, N.B. McKeown, B.S. Ghanem, K.J. Msayib, D. Fritsch, L. Starannikova, N. Belov, O. Sanfirova, Y. Yampolskii, V.J. Shantarovich, Memb. Sci. 325 (2008) 851–860.
[6] Y. Xiao, B.T. Low, S.S. Hosseini, T.S. Chung, D.R. Pai, Prog. Polm. Sci. 34 (2009) 561–580.
[7] Y. Yampolskii, Macromolecules 45 (2012) 3298–3311.
[8] D.F. Sanders, Z.P. Smith, R. Guo, L.M. Robeson, J.E. McGrath, D.R. Paul, B.D. Freeman, Polymer 54 (2013) 4729–4761.
[9] H. Lin, B.D. Freeman, J. Mol. Str. 739 (2005) 57–74.
[10] M. Yoshino, K. Ito, H. Kita, K.J. Okamoto, Polym. Sci. Part B Polym. Phys. 38 (2000) 1707–1715.
[11] Y. Xiao, L. Zhang, L. Xu, T.J. Chung, Memb. Sci. 521 (2017) 65–72.
[12] X. Jiang, S. Li, L. Shao, Energy Environ. Sci. 10 (2017) 1339–1344.
[13] T. Welton, Chem. Rev. 99 (1999) 2071–2084.
[14] P. Scovazzo, J. Kieft, D.A. Finan, C. Koval, D. Dubois, R.D. Noble, J. Membr. Sci. 238 (2004) 57–63.
[15] P. Scovazzo, D. Camper, J. Kieft, J. Poshusta, C. Koval, R.D. Noble, Ind. Eng. Chem. Res. 43 (2004) 6855–6860.
[16] P.K. Kilaru, R.A. Condemarin, P. Scovazzo, Ind. Eng. Chem. Res. 47 (2004)

900–909.
[17] P.K. Kilaru, P. Scovazzo, Ind. Eng. Chem. Res. 47 (2004) 910–919.
[18] S. Raeissi, C.J. Peters, Green Chem. 11 (2009) 185–192.
[19] J.E. Bara, T.K. Carlisle, C.J. Gabriel, D. Camper, A. Finotello, D.L. Gin, R.D. Noble, Ind. Eng. Chem. Res. 48 (2009) 2739–2751.
[20] J.E. Bara, S. Lessmann, C.J. Gabriel, E.S. Hatakeyama, R.D. Noble, D.L. Gin, Ind. Eng. Chem. Res. 46 (2007) 5397–5404.
[21] J.E. Bara, C.J. Gabriel, E.S. Hatakeyama, T.K. Carlisle, S. Lessmann, R.D. Noble, D.L. Gin, J. Membr. Sci. 321 (2008) 3–7.
[22] J.E. Bara, D.L. Gin, R.D. Noble, Ind. Eng. Chem. Res. 47 (2008) 9919–9924.
[23] J.E. Bara, E.S. Hatakeyama, D.L. Gin, R.D. Noble, Polym. Adv. Tech. 19 (2008) 1415–1420.
[24] T.K. Carlisle, E.F. Wiesenauer, G.D. Nocpdemus, D.L. Gin, R.D. Noble, Ind. Eng. Chem. Res. 52 (2013) 1023–1032.
[25] W.M. McDannel, M.G. Cowan, T.K. Carlisle, A.K. Swanson, R.D. Noble, D.L. Gin, Polymer 55 (2014) 3305–3313.
[26] I. Kammakakam, H.W. Kim, S.Y. Nam, H.B. Park, T.H. Kim, Polymer 54 (2013) 3534–3541.
[27] I. Kammakakam, S.Y. Nam, T.H. Kim, RSC Adv. 6 (2016) 31083–31091.
[28] b Gye, I. Kammakakam, H. You, S.Y. Nam, T.H. Kim, Separ. Purif. Tech. 179 (2017) 283–290.
[29] K. Sakaguchi, H. Ito, T. Masuda, T. Hashimoto, Polymer 54 (2013) 6709–6715.
[30] K. Sakaguchi, T. Hashimoto, Polym. J. 46 (2014) 391–398.
[31] A.S. Rewar, R.S. Bhavsar, K. Sreekumar, U.K. Kharul, J. Membr. Sci. 481 (2015) 19–27.
[32] S.V. Shaligram, P.P. Wadgaonkar, U.K. Kharul, J. Membr. Sci. 493 (2015) 403–413.
[33] Y. Nagase, T. Ando, C.M. Yun, React. Func. Polym. 67 (2007) 1252–1263.
[34] C.M. Yun, Y. Saito, Y. Nagase, Trans. Mater. Res. Soc. Jpn. 32 (2007) 1239–1242.
[35] C.M. Yun, Y. Nagase, Proc. Schl. Eng. Tokai Univ. Ser. E 33 (2008) 1–8.
[36] Y. Saito, C.M. Yun, H. Ishikura, Y. Nagase, Trans. Mater. Res. Soc. Jpn. 34 (2009) 145–148.
[37] C.M. Yun, A. Abeta, S. Wirittichai, K. Yamamoto, H. Ishikura, Y. Nagase, Trans. Mater. Res. Soc. Jpn. 35 (2010) 237–240.
[38] C.M. Yun, E. Akiyama, T. Yamanobe, H. Uehara, Y. Nagase, Polymer 103 (2016) 214–223.
[39] Y. Okamura, K. Kabata, M. Kinoshita, D. Saitoh, S. Takeoka, Adv. Mater. 21 (2009) 4388–4392.
[40] K. Yamamoto, S. Suzuki, Y. Saito, C.M. Yun, Y. Nagase, Proc. Schl. Eng. Tokai Univ. Ser. E 38 (2013) 1–8.
[41] L.M. Robeson, J. Membr. Sci. 320 (2008) 390–400.
[42] Y. Osada, T. Nakagawa, Membrane Science and Technology, CRC Press, Boca Raton, FL, 1992.